

This article was downloaded by: [National Chiao Tung University 國立交通大學]

On: 28 April 2014, At: 05:21

Publisher: Taylor & Francis

Informa Ltd Registered in England and Wales Registered Number: 1072954 Registered office: Mortimer House, 37-41 Mortimer Street, London W1T 3JH, UK



## Separation Science and Technology

Publication details, including instructions for authors and subscription information:

<http://www.tandfonline.com/loi/lst20>

### A Continuous Stirred Tank Reactor Study on Chromic Acid Removal by Ion Exchange

Henry K. S. Tan

<sup>a</sup> Department Of Applied Chemistry , National Chiao Tung University , Hsinchu, Taiwan 30050, Republic Of China.

Published online: 04 Mar 2008.

To cite this article: Henry K. S. Tan (1998) A Continuous Stirred Tank Reactor Study on Chromic Acid Removal by Ion Exchange, Separation Science and Technology, 33:8, 1089-1106, DOI: [10.1080/01496399808545242](https://doi.org/10.1080/01496399808545242)

To link to this article: <http://dx.doi.org/10.1080/01496399808545242>

PLEASE SCROLL DOWN FOR ARTICLE

Taylor & Francis makes every effort to ensure the accuracy of all the information (the "Content") contained in the publications on our platform. However, Taylor & Francis, our agents, and our licensors make no representations or warranties whatsoever as to the accuracy, completeness, or suitability for any purpose of the Content. Any opinions and views expressed in this publication are the opinions and views of the authors, and are not the views of or endorsed by Taylor & Francis. The accuracy of the Content should not be relied upon and should be

independently verified with primary sources of information. Taylor and Francis shall not be liable for any losses, actions, claims, proceedings, demands, costs, expenses, damages, and other liabilities whatsoever or howsoever caused arising directly or indirectly in connection with, in relation to or arising out of the use of the Content.

This article may be used for research, teaching, and private study purposes. Any substantial or systematic reproduction, redistribution, reselling, loan, sub-licensing, systematic supply, or distribution in any form to anyone is expressly forbidden. Terms & Conditions of access and use can be found at <http://www.tandfonline.com/page/terms-and-conditions>

## A Continuous Stirred Tank Reactor Study on Chromic Acid Removal by Ion Exchange

---

HENRY K. S. TAN

DEPARTMENT OF APPLIED CHEMISTRY  
NATIONAL CHIAO TUNG UNIVERSITY  
HSINCHU, TAIWAN 30050, REPUBLIC OF CHINA

### ABSTRACT

Dilute chromic acid removal by anion exchange was studied using a continuous stirred tank reactor (CSTR) system. A rate model based on film diffusion control was formulated for quantitative study on the chromate removal. For simplicity, the rate and mass balance equations were formulated for total Cr(VI) concentration. Equations were derived for the effluent concentration history as well as the time-dependent Cr(VI) concentration in the resin. The derived equations for solid and liquid phase Cr(VI) concentration variations were tested and verified by the experimental results obtained. Effects of various operating conditions, such as resin size, feed concentration, and flow rate, were also discussed.

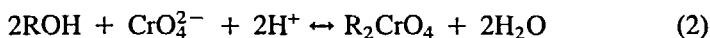
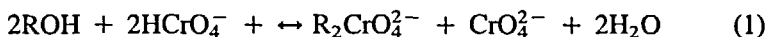
### INTRODUCTION

Ion exchange is now widely used for treating waste rinsewater from the electroplating process. The treatment of dilute rinsewater from the chrome plating process by ion exchange has several advantages over alternative methods. The treated water not only can meet the EPA discharged standard but can also be recycled for the rinsing purpose if desire. In addition, it is possible to recover the chromates stripping from the rinsewater by regenerating the anion-exchange bed. Concentrated chromic acid is obtained after subsequent treatment of the regenerated solution with a cation-exchange bed of hydrogen form. Thus a complete closed system without discharge of the toxic Cr(VI) compound to the environment can be achieved. The practice of treating chrome plating rinsewater by ion exchange started in the early 1940s (1). For the last few decades there have been continuous studies (2–7) in this area.

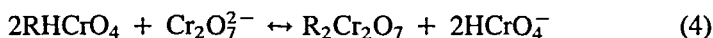
However, very few studies have been made on the kinetics of chromic acid removal by ion exchange. An understanding on the rate of chromate uptake on an anion-exchange resin is essential in the application of treatment of chromium plating rinsewater by the ion-exchange method. Although most ion-exchange processes are conducted in a fixed bed, quantitative analysis of the column dynamics is very complex compared to batch (8–10) or CSTR systems (11). The batch runs are usually conducted under nonflow condition, in contrast to the constant flow of feed solution through the column in fixed-bed processes. The use of a CSTR system not only facilitates quantitative analysis but also enables operation under flow condition. For dilute solutions in which film diffusion tends to be the rate-controlling step, the film thickness depends on both the flow rate and the degree of agitation in the CSTR. In the case of fixed-bed operation, film thickness depends primarily on the flow rates employed. By employing a CSTR system and using a linear rate expression, rate parameters can be evaluated readily from experimental results. The values of rate parameter obtained can then be compared with those obtained from correlations which are often used in the design of column operation.

### MECHANISM OF CHROMATE UPTAKE AND RATE OF EXCHANGE

The removal of dilute chromic acid by ion exchange involves the reaction and exchange of several chromate ionic species with an anion exchanger of the OH form. According to a study carried out by Arden and Giddings (12), the first stage of exchange and reaction involves the conversion of the OH ion in the resin to its monochromate form. Only when all the OH group in the resin are consumed will further conversion to the dichromate form proceed. The first stage of exchange includes the following equations:



These two reactions terminate only when all  $\text{OH}^+$  ions attached to the resin are consumed and converted to the  $\text{R}_2\text{CrO}_4$  form. Thus, at the end of the first stage of exchange, the Cr(VI) content in the resin will be half of the resin capacity. The second stage of exchange involves the ordinary exchange between  $\text{HCrO}_4^-$ ,  $\text{CrO}_4^{2-}$ , and  $\text{Cr}_2\text{O}_7^{2-}$ . The exchange reactions are expected to proceed as follows:



In the second stage of reaction, the total solution concentration decreases as long as more of the  $R_2CrO_4$  form of the resin is converted to either  $R_2CrO_7$  or  $RHCrO_4$ . The total amount of Cr(VI) decreases since for every 2 moles of  $R_2CrO_4$  converted, 1 mole of Cr(VI) is removed from the solution.

The composition of various chromate species present in dilute chromic acid solution depends on the total Cr(VI) concentration and also on the pH of the solution. The distribution of various chromates present can be determined from equations based on charge balance, total Cr(VI) mass balance, and dissociation equilibrium expressions (13). It is assumed that no other electrolytes are present aside from various chromate species, and that the activity coefficient is unity since the solution is very dilute. For a concentration of chromic acid between 0.1 to 0.4 g/L  $CrO_3$  and for a pH between 2.5 to 5.5, calculations indicated that the predominant species present is  $HCrO_4^-$ . It is now generally accepted that ion exchange is a diffusion rate-controlling process. For a dilute solution, film diffusion is likely the rate-controlling step (14). For ease of quantitative analyses, rate equations will be formulated only for total Cr(VI) rather than the various individual chromate species. Using the linear driving force rate expression for film diffusion

$$dq/dt = k_f a_p (C - C^*) \quad (5)$$

where  $k_f$  is the mass transfer coefficient on the liquid side,  $a_p$  is the mass transfer area per unit volume of resin particle, and  $q$  and  $C$  denote the total Cr(VI) concentration in the resin and in the solution, respectively.  $C^*$  is the liquid film Cr(VI) concentration in equilibrium with the resin. This simple form of the rate equation is used together with the conservation of mass equation for the quantitative study of the CSTR system.

## QUANTITATIVE STUDY OF CSTR SYSTEM

The mass balance for the CSTR system is

$$F(C_{in} - C) = V_r \frac{dq}{dt} + V \frac{dC}{dt} = 0 \quad (6)$$

where  $F$  is the volumetric flow rate,  $C_{in}$  is the concentration of Cr(VI) in the feed solution,  $V_r$  is the volume of the resin, and  $V$  is the volume of solution in the CSTR.

For experimental work carried out in this study, the term  $V(dC/dt)$  in Eq. (6) is small compared to  $V_r(dq/dt)$  and the mass balance can be approximated by

$$F(C_{in} - C) = V_r \frac{dq}{dt} \quad (7)$$

Introducing dimensionless concentration variables  $x$  and  $y$  to the differential mass balance equation for total Cr(VI):

$$R \frac{dy}{dt} = (1 - x) \quad (8)$$

where  $x = C/C_{in}$ ,  $y = q/Q_c$ , and  $R = V_r Q_c / FC_{in}$ .

Analogous to a fixed-bed ion-exchange system, a dimensionless time variable in terms of  $T$  can also be used instead of an absolute time variable. The throughput variable  $T$  is defined by  $T = t/R$ . To grasp the significance of  $R$ , the quantity  $R$  can be viewed as a stoichiometric throughput time parameter. In other words, at time equal to  $R$ , a stoichiometric amount of Cr(VI) in the solution has been passed through the CSTR.

Using the dimensionless concentration variables, the corresponding rate equation is

$$\frac{dy}{dt} = \frac{k_f a_p C_{in}}{Q_c} (x - x^*) \quad (9)$$

The resulting equation from solving simultaneously rate and mass balance expressions is

$$x = \frac{1 + ax^*}{1 + a} \quad (10)$$

where  $a = Wk_f a_p / F\rho = V_r k_f a_p / F$ ,  $W$  is the weight of resin, and  $\rho$  is the density of the resin.

In the case in which the value of  $x^*$  is negligible or is small compared to the value of  $x$ , a situation which is valid during the early stage of exchange, Eq. (10) become

$$x = \frac{1}{1 + a} \quad (11)$$

Substituting Eq. (10) for the value of  $x$  in the rate equation and simplifying:

$$\frac{dy}{dt} = \frac{k_f a_p C_{in}}{Q_c(1 + a)} (1 - x^*) \quad (12)$$

The integration of Eq. (12) requires the equilibrium relationship of  $x^*$  and  $y$  which was independently obtained experimentally in this work and is shown in Fig. 1.

The variation of  $y$  with time can thus be obtained numerically by substituting  $x^*$  for  $y$  in Eq. (12). Once  $y(t)$  or  $x^*(t)$  is known,  $x(t)$  can then be determined from Eq. (10). Alternately, with the initial value of  $y = 0$  and  $x =$

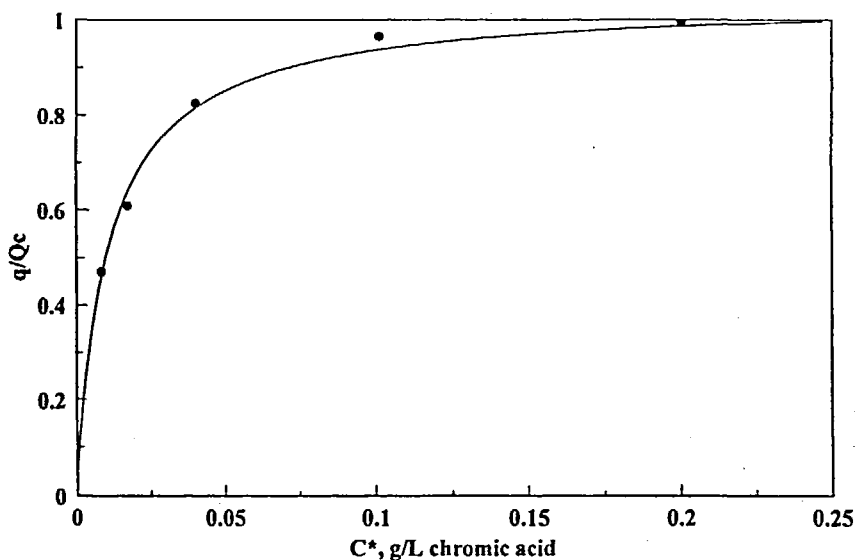


FIG. 1 Equilibrium relation of  $C^*$  and  $q/Q_c$ .

0, for a small increment of  $t$ , the value of  $y(t)$  can be calculated numerically using the differential mass balance of Eq. (8) together with the equilibrium relation of  $x^*$  and  $y$ .

In addition to deriving  $x(t)$  and  $y(t)$ , it is worthwhile to develop equations that can predict the effluent pH as the exchange proceeds. The simplest approach is to assume that all the chromates are present as  $\text{HCrO}_4^-$ . In this case the effluent  $\text{HCrO}_4^-$  concentration is also the effluent Cr(VI) concentration. The effluent pH can then be easily calculated with a charge balance once the value of effluent Cr(VI) concentration is known. A more rigorous calculations involved the assumption of the presence of  $\text{CrO}_4^{2-}$  and  $\text{Cr}_2\text{O}_7^{2-}$  in addition to  $\text{HCrO}_4^-$ . The effluent pH can then be calculated by the total Cr(VI) balance, the charge balance, and the following two ionic dissociation equilibrium expressions (15):

$$K_1 = \frac{[\text{H}^+][\text{CrO}_4^{2-}]}{[\text{HCrO}_4^-]} = 3.2 \times 10^{-7} \quad (13)$$

$$K_2 = \frac{[\text{Cr}_2\text{O}_7^{2-}]}{[\text{HCrO}_4^-]^2} = 0.0302 \quad (14)$$

## EXPERIMENTAL

### Experimental System

Dilute chromic acid solutions of concentration ranging between 0.1 to 0.4 g/L  $\text{CrO}_3$  were prepared for the experimental work. This level of concentration is very close to that of the chrome plating rinsewater discharged. Strong anion resins, Dowex 1-X8, were used in the study. A 65-mL beaker was employed for the experimental CSTR runs, and a magnetic stirrer was used for agitation. The beaker is equipped with inlet and outlet tubes. Experimentally, it is not possible to analyze the various chromate species separately. Instead, the analysis was carried out only for the total Cr(VI) concentration in the solution. The study of the kinetics of ion exchange is usually applied to a binary system with two counterions. For an ordinary exchange process where no chemical reaction is involved, the total ionic concentration is constant. Thus, knowing the concentration of one species of counterion automatically determines the concentration of the other. In the case of this study, the total ionic concentration is not constant owing to the neutralization involved. Many of the experimental studies on kinetics of ion exchange present results based on the concentration changes in the resin phase. In this work the experimental value of Cr(VI) concentration in the resin was determined from the measured Cr(VI) concentration in the solution by means of an integral mass balance. In a batch system, if the resin phase concentration can be measured directly, a very large volume of solution is used relative to the amount of resin employed. This enables the use of the infinite volume model and the application of a constant resin surface concentration assumption. In the CSTR system, although the feed concentration is constant, both the exchanger surface composition and the instantaneous solution concentration are changing with time.

### Resin Capacity Determination and Analytical Methods

Three different sizes of Dowex 1-X8 resin were used in the experimental study. These were sizes with mesh numbers. 20–50, 50–100, and 100–200. The resin was originally in chloride form and was converted to the  $\text{OH}^-$  form by the standard procedure. The three different size resins were also determined for their capacities.

For the analytic work, the pH of the chromic acid solution was directly measured by a pH meter. The analysis for  $\text{Cl}^-$  in the capacity determination was by titration with  $\text{AgNO}_3$  solution. A spectrophotometric method was used to analyze the total Cr(VI) concentration for the feed and effluent solution. This method is based on the principle that the Cr(VI) present in solution reacts with 1,5-diphenylcarbazine to form purple reddish matter. The amount of this substance formed was then determined quantitatively from the amount



of absorbance with the wavelength of the spectrophotometer set at 540 nm. This method is applicable for a Cr(VI) concentration range of 0.1 to 1 mg/L CrO<sub>3</sub>.

### Experimental Procedure

For each experiment the 65-mL beaker CSTR was filled with 50 mL of distilled water. A specified amount and a specified type of Dowex 1 resin were introduced to the beaker. The prepared known chromic acid solution was fed to the beaker at a constant flow rate. The effluent was also maintained at the same flow rate as that of the feed. The effluent Cr(VI) concentration and pH were measured at a time interval of about 5 to 10 minutes. All the experimental runs were terminated only when the effluent Cr(VI) concentration was close to the final steady-state value.

### RESULTS AND DISCUSSION

Experimental runs were performed for a continuous stirred tank reactor (CSTR) system in which Dowex 1-X8 resins in a 65-mL vessel were in continuous contact with a constant feed solution of dilute chromic acid. The operating conditions of these experimental runs are listed in Table 1. The aims of these experiments were to determine the values of the rate parameters and the effects of various operating conditions on the rate of removal of chromic acid in a flow system. The rate parameter,  $k_r a_p$ , is related to  $3D/\delta r_0$  after applying Fick's law. Here  $D$  is the effective diffusion coefficients for ions

TABLE I  
Operating Conditions for CSTR Runs

Run	$W$ (g)	$F$ (mL/m)	$C$ (g/L)	$Q'_c$ (meq/g)	$r_0$ (mesh no.)	Stirring rate (rpm)
1	5.033	50.1	0.1016	3.446	20-50	335
2	5.044	50.1	0.1932	3.446	20-50	335
3	5.005	50.1	0.4159	3.446	20-50	335
4	5.066	40.1	0.1925	3.446	20-50	335
5	5.087	80.2	0.1932	3.446	20-50	335
6	4.008	50.1	0.1946	3.446	20-50	335
7	6.047	50.1	0.1991	3.446	20-50	335
8	5.066	50.1	0.1972	3.446	20-50	620
9	5.005	50.1	0.1965	3.446	20-50	905
10	5.005	50.1	0.1961	3.607	50-100	335
11	5.001	50.1	0.2001	3.756	100-200	335

in the solution,  $\delta$  is the film thickness, and  $r_0$  is the resin radius. Table 2 lists the value of  $k_f a_p$  and  $D/\delta r_0$  as calculated from experimental data. In kinetics experiments carried out in a shallow bed or batch system, the resin will eventually come to equilibrium with respect to the solution concentration employed. In a CSTR system the final steady state is reached when the effluent solution concentration approaches that of the feed. The final resin Cr(VI) concentration is the value that is in equilibrium with respect to the feed solution concentration of Cr(VI). For feed concentration Cr(VI) higher than 0.1 g/L CrO<sub>3</sub>, experimental results showed that the resin will be converted entirely to the dichromate or hydrogen chromate forms. Realization of the ultimate dichromate capacity is an important element in the quantitative interpretation of experimental data. The experimental results obtained in this study were used to check the theoretical equations derived. These results were also used in discussing the parametric effect related to the rate of exchange. These operating parameters include the feed concentration, flow rate, size of the resin, amount of resin used in the vessel, and the degree of agitation in the CSTR.

In conjunction with the values of rate parameters calculated and listed in Table 2, it is worthwhile to consider how they can related to the design of fixed-bed processes. For column operation, Glueckauf (16) recommended that the mass transfer coefficient for the film diffusion rate controlled be calculated by  $k_f = 3D/2\delta r_0$ . Glueckauf also gave the following correlation for calculating film thickness:

$$\delta = \frac{r_0}{5(1 + 70r_0 V_s)}$$

where  $V_s$  is the linear superficial flow rate for column runs. Owing to pressure drop consideration, resin sizes used for fixed-bed runs are usually of 20–50 mesh. The flow rates employed are as low as 1 gpm/ft<sup>2</sup> (0.07 cm/s) for regeneration and as high as 30 gpm/ft<sup>2</sup> (2 cm/s) for treating a dilute solution. For a  $r_0$  value of about 0.03 cm (20–50 mesh) and with a linear superficial flow rate of 0.3 to 2 cm/s (4 to 30 gpm/ft<sup>2</sup>), the value of  $\delta/r_0$  calculated from

TABLE 2  
Values of  $k_f a_p V_r / F$  and  $D/\delta r_0$  Determined from CSTR Runs

	Run										
	1	2	3	4	5	6	7	8	9	10	11
$k_f a_p V_r / F$	3.01	4.13	3.10	4.56	2.85	2.78	4.40	3.92	5.16	23.7	82.6
$k_f a_p, s^{-1}$	0.449	0.615	0.465	0.541	0.674	0.521	0.547	0.589	0.776	3.56	12.4
$D/\delta r_0$	0.150	0.205	0.155	0.180	0.225	0.174	0.182	0.196	0.259	1.19	4.13

Glueckauf's correlation is in the 0.04 to 0.12 range. An estimate of the value of effective diffusivity is needed to determine values of  $\delta/r_0$  from the CSTR data. Since  $\text{HCrO}_4^-$  is the predominant chromate species present and neutralization takes place when  $\text{OH}^-$  is released from the resin,  $D$  can be calculated by (17)

$$D = \frac{2D_{\text{H}^+}D_{\text{HCrO}_4^-}}{D_{\text{H}^+} + D_{\text{HCrO}_4^-}}$$

where  $D_{\text{H}^+}$  and  $D_{\text{HCrO}_4^-}$  are the self-diffusion coefficients of the hydrogen ion and the hydrogen chromate ion, respectively. With a value of  $D_{\text{H}^+} = 9.3 \times 10^{-5} \text{ cm}^2/\text{s}$  (18) and assuming  $D_{\text{HCrO}_4^-} = 1 \times 10^{-5} \text{ cm}^2/\text{s}$ , the calculated value of  $D$  is equal to  $1.8 \times 10^{-5} \text{ cm}^2/\text{s}$ . From Table 2 the values of  $\delta/r_0$  for Runs 1 to 9 were calculated to be in the range of 0.07 to 0.13. The film thickness resulting from employing these flow condition and the stirring rates in Table 1 for these 9 runs is very close to that of conducting fixed-bed runs with a superficial flow rate set between 4 to 13 gpm/ft<sup>2</sup>.

### Comparisons of Calculated and Experimental Results

As mentioned in the experimental Section, the experimental value of  $q(t)$  was determined from measuring the value of  $C(t)$  by means of an integral mass balance. From the theoretical equations derived, if the assumption of neglecting the value of  $C^*$  is valid for the early stage of exchange, the effluent Cr(VI) concentration is expected to be constant up to the time when all the resin are converted from the  $\text{OH}^-$  form to the monochromate form. Similarly, for this same period, the amount of Cr(VI) uptake in the resin varies linearly with time. These characteristics were verified for most of the experimental results obtained. Figure 2 shows the experimental and calculated effluent concentration history for a CSTR system operating at two different flow rates (Runs 2 and 5). The same experimental data are plotted in Fig. 3, which shows the variation of the fraction of resin in the Cr(VI) form with time. Data presented in ion-exchange kinetics studies are usually expressed in terms of fractional attainment of equilibrium versus time. The fractional attainment of equilibrium, designated with symbol  $U(t)$ , is related to the resin phase counterion composition by

$$U_t = \frac{q(t) - q_0}{q^* - q_0}$$

where  $q_0$  is the initial concentration and  $q^*$  is the saturated value with respect to the final solution concentration. From Fig. 1, for a solution concentration greater than 0.1 g/L  $\text{CrO}_3$ ,  $q^*/Q_c$  is approximately equal to unity. In other

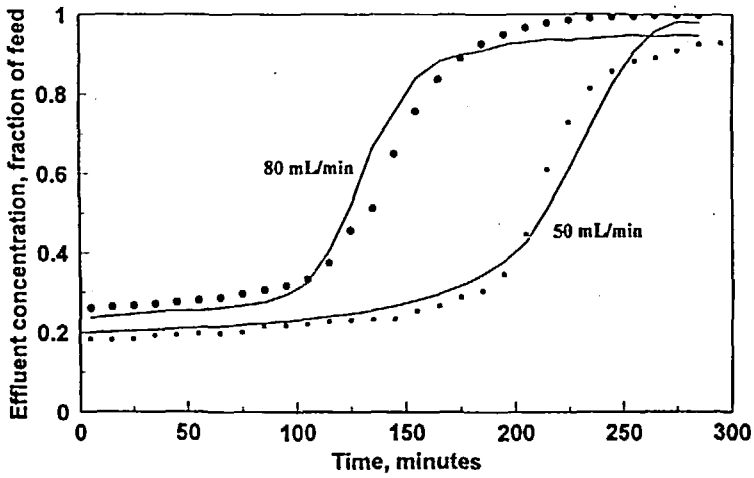


FIG. 2 Experimental and calculated results of effluent concentration history for Runs 2 and 5.

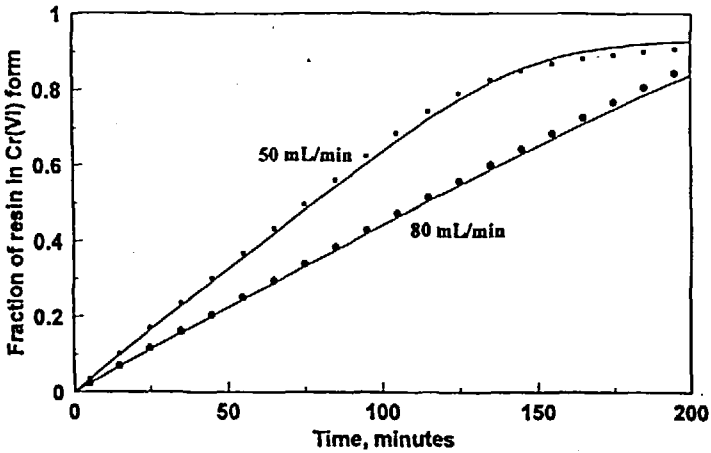


FIG. 3 Experimental and calculated results of variation of fraction of resin in Cr(VI) form with time for Runs 2 and 5.

words, the value of  $q^*$  assumes the value of  $Q_c$ . Thus the  $q/Q_c$  versus  $t$  plot in Fig. 3 can also be interpreted as a  $U(t)$  plot, with the ordinate scale also representing the fractional attainment of equilibrium. To utilize equations derived for the calculation of  $x$  and  $y$  requires the determination of  $k_f a_p$  values. From the early stage of the experimental effluent concentration profile, the value of  $k_f a_p$  can be estimated from

$$\frac{C}{C_{in}} = \frac{k_f a_p C_{in} / Q_c}{1 + V_r k_f a_p / F}$$

which is a constant. Use of Eqs. (10) and (12) and the estimated value of  $k_f a_p$  enables the calculation of  $x$  and  $y$ , which are shown in Figs. 2 and 3. Figures 4 and 5 are experimental and calculated results for runs starting with two different amounts of resin present. There is good agreement between the experimental and calculated results as shown in Figs. 2 to 5. Any discrepancy must be due to experimental error in determining the equilibrium relation and the assumption of constant values of  $k_f a_p$ . It is observed that the deviation is more pronounced in the latter part of the effluent curve. As the resin Cr(VI) concentration increases, diffusion within the resin bead will play a significant role in the overall rate of exchange. Figure 6 shows the experimental and calculated effluent pH for Runs 2 and 5. The calculated values of pH were obtained from knowing the total Cr(VI) concentration and from charge and total mass balances.

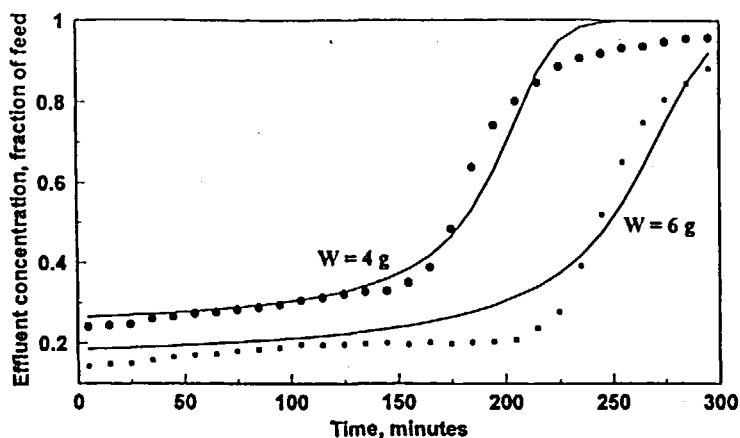


FIG. 4 Experimental and calculated results of effluent concentration history for Runs 6 and 7.

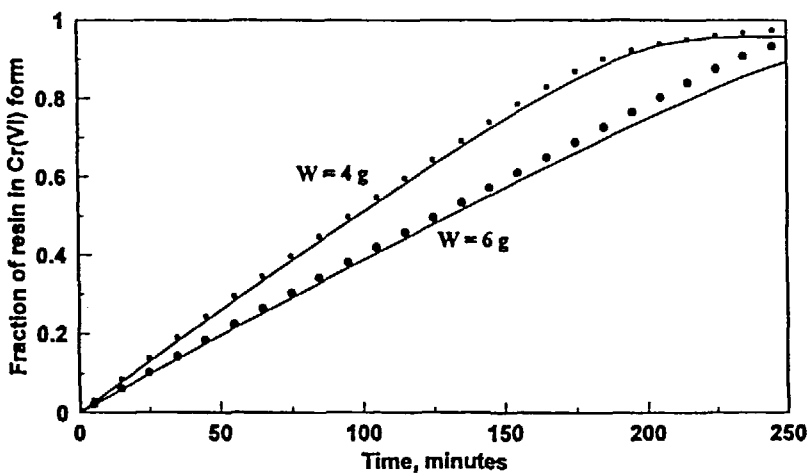


FIG. 5 Experimental and calculated results of variation of fraction of resin in Cr(VI) form with time for Runs 6 and 7.

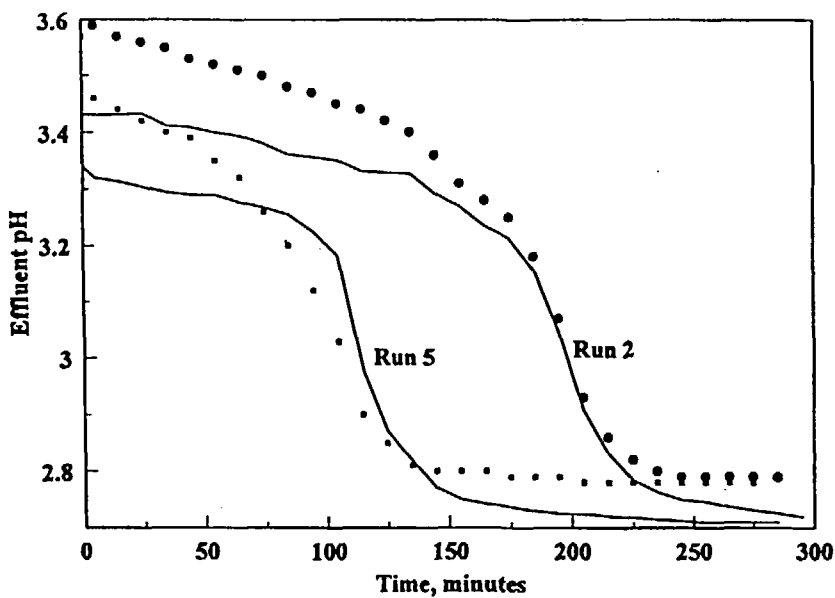


FIG. 6 Experimental and calculated results for effluent pH for Runs 3 and 4.

### Effects of Operating Parameters and Conditions

#### Effect of Feed Concentration

Figures 7 and 8 show the experimental results for Runs 1 to 3. These three runs were conducted using different feed concentrations. The effluent concentration history plot shown in Fig. 7 indicates breakthrough is sharper for the higher feed concentration. From Table 2, the calculated  $k_f a_p$  values for these runs are very close and did not differ more than 30%. The lower rate for resin's conversion to Cr(VI) form as indicated in Fig. 8 must be attributed to the smaller driving force involved. With the same amount of resin capacity used, a lower feed concentration results in employing a higher value of  $R$ , which is equal to  $V_r Q_c / FC_{in}$ . Thus, for the smaller feed concentration run, it is expected that a much longer time will be required for the resin to reach saturation Cr(VI) capacity.

#### Effect of Resin Size

Figures 9 and 10 show experimental results obtained for Runs 2, 10 and 11. The smaller size of resin bead used results in a larger value of  $a_p$ . The calculated  $k_f a_p$  values listed in Table 2 indicate that the value of  $k_f a_p$  for a 100–200 mesh run is about 4 times that of a 50–100 mesh run and almost

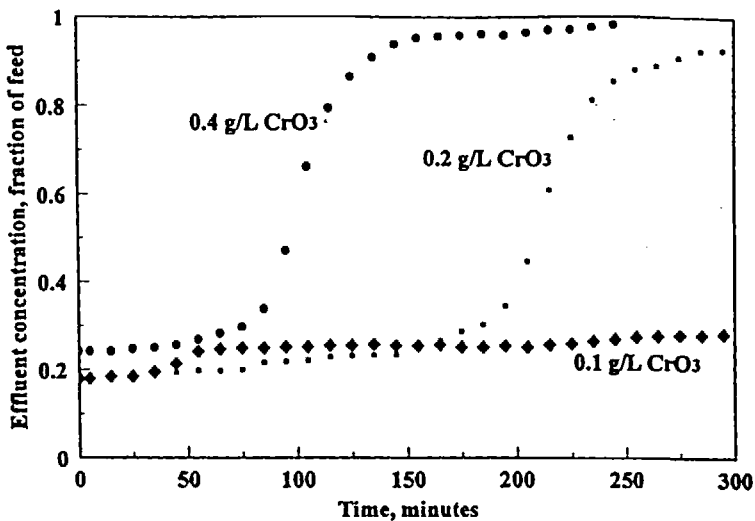


FIG. 7 Experimental results of effluent concentration history for three different feed concentrations.

Downloaded by [National Chiao Tung University] at 05:21 28 April 2014

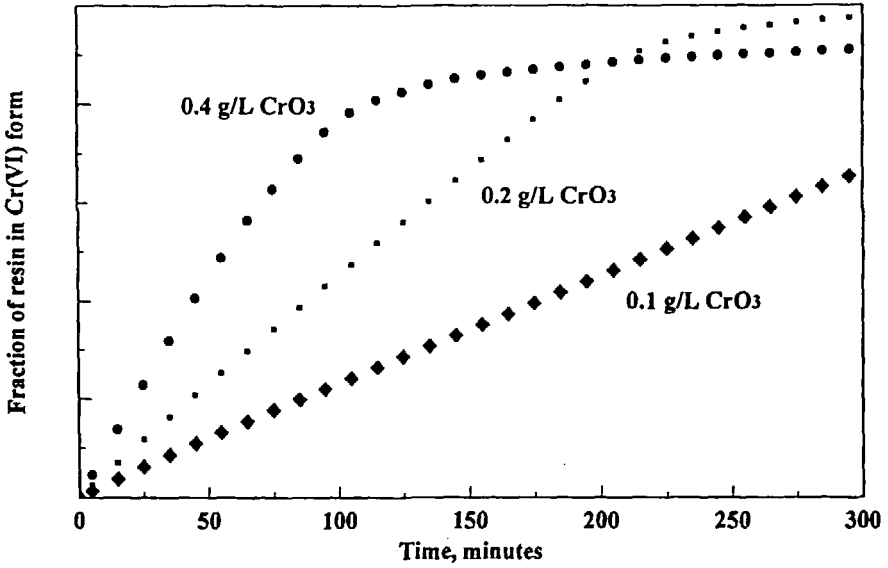


FIG. 8 Experimental results of variation of fraction of resin in Cr(VI) form with time for three different feed concentrations.

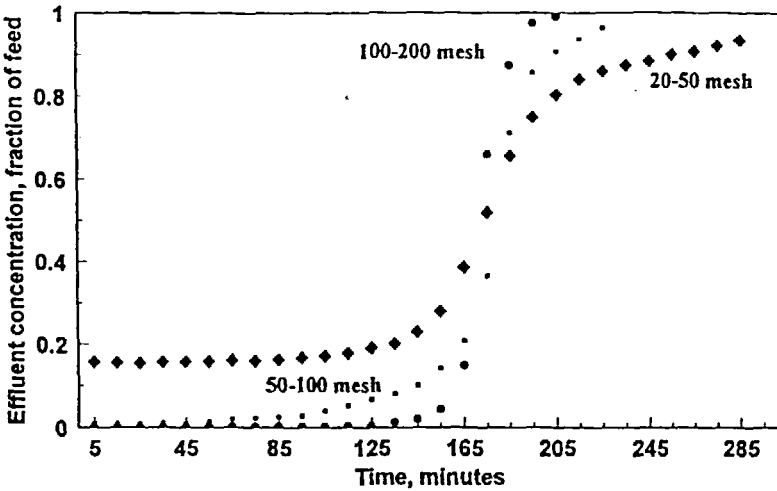


FIG. 9 Experimental results of effluent concentration history for the three different sizes of resin used.



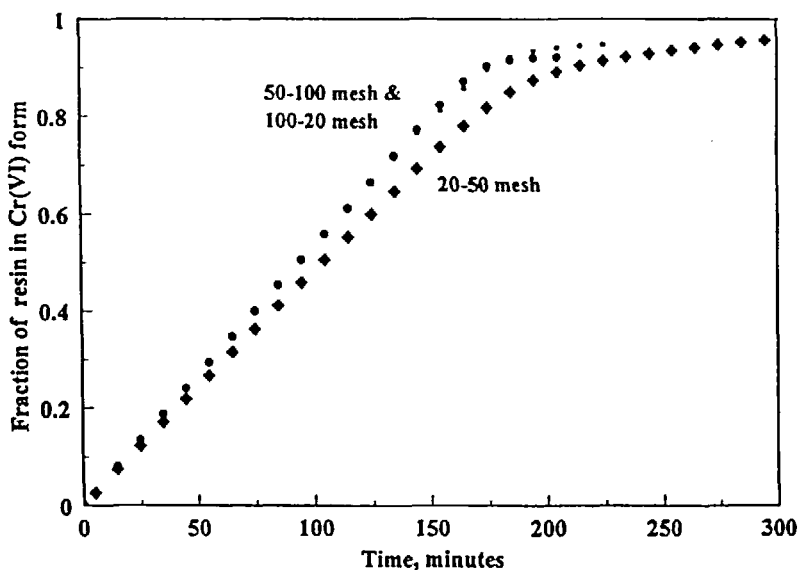


FIG. 10 Experimental results of variation of fraction of resin in Cr(VI) form with time for the three different sizes of resin used.

20 times that of a 20–50 mesh run. It is seen that both 50–100 and 100–200 mesh runs have sharper breakthroughs than the 20–50 mesh run. The sharper breakthrough for a smaller size of resin, as shown in Fig. 9, is to be expected because of the higher rate of exchange due to the increase in transfer area. The extreme high value of  $k_f a_p$  obtained for Runs 10 and 11 indicates that a diminishing resin size effect is approached. This is evident from the results shown in Fig. 10. There is almost no difference with respect to the rate of Cr(VI) take up for 50–100 and 100–200 mesh runs.

### Effect of Flow Rate

A fast feed flow rate is expected to reduce the film thickness and thus result in a higher value of  $k_f$ . This is verified by the values of  $k_f a_p$ , determined from experimental results of Runs 2, 4, and 5, as listed in Table 2. It is seen that the value of  $k_f a_p$  for the 80 mL/min run is about 25% more than the run with a flow rate of 40 mL/min and about 10% more than the 50 mL/min run. In runs with various feed concentrations, both the values of  $k_f a_p$  and the reciprocal of  $R$  are larger for a higher feed concentration. In the case of variation of flow rate runs, a higher flow rate yields a higher value of  $k_f a_p$ .

and at the same time leads to a lower value of  $R$ . From a rate equation consideration, the rate of Cr(VI) uptake in the resin is proportional to the rate parameter. However, from the differential mass balance equation, the rate of Cr(VI) uptake is inversely proportional to the value of  $R$ . As indicated in Fig. 3, the value of  $R$  seems to have a more pronounced effect on the uptake of Cr(VI) in the resin. The value of  $R$  for the 50 mL/min run is 1.6 times that of the 80 mL/min run. In Fig. 2 the effluent concentration for the 50 mL/min run is fairly constant up to a time of about 200 minutes. Thus in Fig. 3 a straight line is obtained for the  $q/Q$  versus  $t$  plot, with the slope equal to the value of  $1/R$ .

### Effect of Stirring Rate

As in the case for flow rate variation, an increase in the speed of the stirrer tends to reduce the film thickness and increases the rate of Cr(VI) loading in the resin. However, as pointed out by Helfferich (14), agitation speed can only reach a certain hydrodynamic efficiency, beyond which a further increase will have no effect on the kinetics of ion exchange. It is seen from Fig. 11, which is a plot of the effect of stirrer speed on the rate of uptake of Cr(VI) in the resin, that the maximum hydrodynamics efficiency is approached when

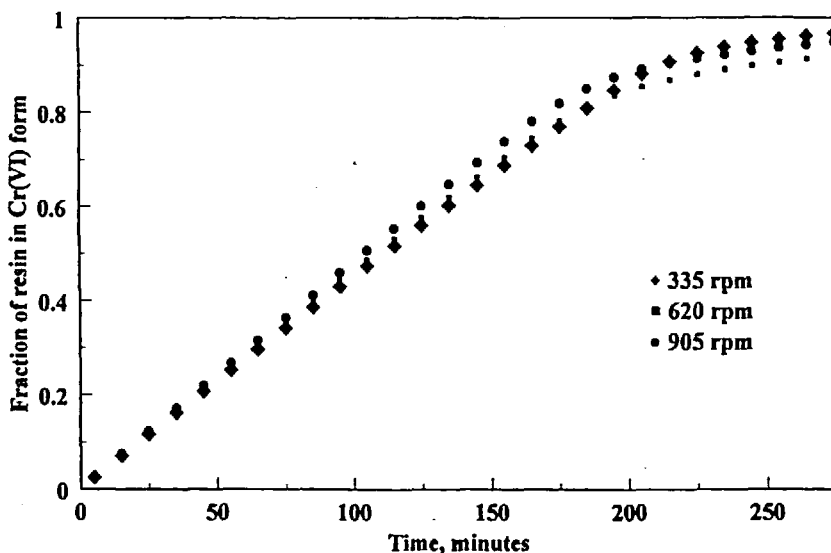


FIG. 11 Experimental results of variation of fraction of resin in Cr(VI) form with time for three different stirring rates in the CSTR.

the stirrer is operating at 905 rpm. In any case, the results show that there is no substantial difference in the rate of Cr(VI) uptake for the 303 and 605 rpm runs.

### ***Effect of Amount of Resin Present in CSTR***

The values of  $k_t a_p$  obtained for Runs 6 and 7 were very close. The higher rate of conversion of resin to the Cr(VI) form for the 4 g resin run, as indicated in Fig. 5, is due to the smaller value of the stoichiometric throughput time parameter  $R$ . The ratio of  $R$  for the 6 g resin run to that of the 4 g resin run is about 1.5. It is seen in Fig. 4 that the 6 g resin runs give a lower breakthrough than the 4 g resin runs. This is due to the fact that the more the total exchanger capacity present, the more the amount of Cr(VI) in the solutions will be removed from the solution.

## **CONCLUSIONS**

In this study, kinetics of chromic acid removal by ion exchange were conducted in a CSTR system. The dilute  $\text{CrO}_3$  solution employed in the experimental work justified the use of a film diffusion rate control model for quantitative analysis. For simplicity and ease of quantitative study, the rate and mass balance expressions were formulated for total Cr(VI) concentration. Equations were derived for the effluent concentration history as well as the time-dependent Cr(VI) concentration in the resin. The derived equations indicated that the rate of uptake of Cr(VI) depends on both a kinetic parameter and a stoichiometric throughput time parameter. The derived equations were tested and verified by the experimental results obtained. The effects of various operating conditions on the rate of removal of chromic acid are caused by several factors. When a small-sized resin is used, the rate increases because of the increase in the mass transfer area. The rate increase for a high stirring rate is due to the reduction of film thickness. With regard to the effects of flow rate and feed concentration, the rate of Cr(VI) removal depends on both the magnitude of the rate parameter and the stoichiometric throughput time parameter.

## **SYMBOLS**

$a_p$	mass transfer surface area ( $\text{cm}^2/\text{cm}^3$ )
$C$	concentration of Cr(VI) in solution (g/L or meq/L)
$C_{\text{in}}$	feed Cr(VI) concentration to CSTR (g/L or meq/L)
$C^*$	equilibrium Cr(VI) concentration in solution (g/L)
$D$	effective diffusivity of ions in solution ( $\text{cm}^2/\text{s}$ )

$F$	volumetric flow rate of solution (mL/min)
$k_f$	mass transfer coefficient on liquid side (cm/s)
$q$	concentration of Cr(VI) in resin (meq/mL)
$Q_c$	capacity of the resin, wet basis (meq/mL)
$Q'_c$	capacity of the resin, dry basis (meq/g)
$r_0$	resin bead radius, cm
$R$	stoichiometric throughput time parameter (minutes)
$t$	absolute time (seconds)
$U$	fractional attainment of equilibrium
$V$	volume of solution in CSTR (mL)
$V_s$	linear superficial flow rate in fixed bed (cm/s)
$V_r$	volume of resin in CSTR (mL)
$W$	weight of resin (g)
$x$	dimensionless Cr(VI) concentration in solution
$y$	dimensionless Cr(VI) concentration in the resin

### Greek Letter

$\delta$	film thickness (cm)
----------	---------------------

### REFERENCES

1. S. Sussman, F. C. Nachold, and W. Wood, *Ind. Eng. Chem.*, **37**, 618 (1945).
2. R. L. Costa, *Ibid.*, **42**, 308 (1950).
3. J. M. Culotta and W. F. Swanton, *Plating*, **57**, 251 (1970).
4. H. Gold, in *Ion Exchange for Pollution Control*, Vol. I (C. Calmon and H. Gold, Eds.), CRC Press, Boca Raton, FL., 1979, Chapter 14
5. B. Mulvaney, *Plating*, **61**, 544 (1974).
6. L. Pawlowski, B. Klepacka, and R. Zaleski, *Water Res.*, **15**, 1153 (1981).
7. T. Nadeau and M. Dejak, *Plat. Surf. Finish.*, **73**(4), 48 (1986).
8. R. A. Blickenstaff, J. D. Wagner, and J. S. Dranoff, *J. Phys. Chem.*, **71**, 1665 (1967).
9. R. A. Blickenstaff, J. D. Wagner, and J. S. Dranoff, *Ibid.*, **71**, 1670 (1967).
10. E. E. Graham and J. S. Dranoff, *AIChE J.*, **18**, 608 (1972).
11. J. M. Marchello and M. W. Davis Jr., *Ind. Eng. Chem., Fundam.*, **2**, 27 (1963).
12. T. V. Arden and M. Giddings, *J. Appl. Chem.*, **11**, 229 (1961).
13. A. K. Sengupta and L. Lim, *AIChE J.*, **34**, 2019 (1988).
14. F. Helfferich, *Ion Exchange*, McGraw-Hill, New York, NY, 1962, Chapter 6.
15. J. N. Butler, *Ionic Equilibrium, A Mathematical Approach*, Addison-Wesley, New York, NY, 1964
16. E. Glueckauf, in *Ion Exchange and Its Applications*, Society of Chemical Industry, London, 1955, pp. 34–46.
17. F. Helfferich, in *Ion Exchange* (L. A. Marinsky, Ed.), Dekker, New York, NY, 1966, Chapter 2.
18. E. I. Cussler, *Diffusion: Mass Transfer in Fluid Systems*, Cambridge University Press, New York, NY, 1984, Chapter 6.

Received by editor May 25, 1997

Revision received of September 1997